

# Thermal stabilization of catalytic compositions for automobile exhaust treatment through rare earth modification of alumina nanoparticle support

Masakuni Ozawa\*

*Ceramics Research Laboratory, Nagoya Institute of Technology, Tajimi, 507-0071 Gifu, Japan*

Received 30 July 2004; received in revised form 25 November 2004; accepted 15 December 2004

Available online 28 June 2005

## Abstract

The relationship of materials design and thermal stabilization of catalysts is discussed by focusing on a series of useful rare earth elements used in automotive catalysts. In general, automobile exhaust becomes a high-temperature gas after the engine operation. The thermal durability is very important in any case of practical usage concerning with the exhaust catalyst. The catalysis, i.e., complex reactions between gases, must be discussed about the catalytic materials subjected to such harsh heat condition. Rare earth elements, in the design of advanced catalysts, are essential to the requirement of heat-stable catalytic materials as well as other function including oxygen storage capacity. For the alumina catalytic support, the phase transition and surface modification are closely related to realize better heat-stable materials with nanometer-order particles in size. The thermal-stable alumina support and the oxygen storage capacity (OSC) of ceria and ceria–zirconia subcatalysts must be controlled by the resultant microstructures where the nanoparticles are mixed and rearranged with each other after heat treatment. The materials aspect for the design of automotive catalyst is reviewed, and then the author's work on the use of rare earth elements as key technology is described.

© 2005 Elsevier B.V. All rights reserved.

*Keywords:* Automotive catalyst; Alumina support; Oxygen storage capacity; NO<sub>x</sub>; Thermal stability

## 1. Introduction

Automotive exhaust catalysts are used for treatment to remove poison gases, such as CO, hydrocarbons and NO<sub>x</sub> in burning exhaust from engines. Regarding with materials design in the practical use of catalysts, rare earths are the most important elements to meet several requirement of exhaust treatment so far [1,2]. In practical development, the thermal stabilization has become essential factors to control the state of catalysts from aspect of nanoscaled composite of several catalytic compositions. In general, the automotive catalysts consist of precious metals including Pt, Rh and Pd, alumina nanoparticles as supports, and subcatalytic composition such as ceria or ceria–zirconia as well as other promoters. Although the inexpensive materials, especially

alumina support [3–9] and rare-earths-containing subcatalysts [10–15] have been examined through more advanced technology, their effective application requires both better properties and lower cost level for advanced automotive catalyst. Also, a recent research has lead new compositions, such as Pd-doped perovskite-type oxides mixed with ceria-based subcatalyst, in order to avoid the use of expensive Pt–Rh [16–19]. In the present paper, the rare earth modification to alumina is described for furthering more research of thermal-resistant catalyst. The thermal stabilization effect of a series of rare earth elements on alumina support is examined by observing the surface area and phase transition in metastable gamma alumina. Then, the sintering in alumina supported ceria–zirconia system and the effect of lanthanum on transition metal impregnated alumina on phase transition and the stabilized copper–alumina are examined for de-NO<sub>x</sub> catalyst without precious metals for lean burn exhaust. In addition, the morphology stabilization of alumina coat layers is shown.

\* Tel.: +81 572 27 6811; fax: +81 572 27 6812.  
E-mail address: ozawa@nitech.ac.jp.

These results suggest the high potential of rare earth modification technology to alumina-based catalyst. The present work emphasizes the importance of rare earths and their arrangement in these catalytic components.

## 2. Experimental

A series of rare earths (RE = La, Ce, Sm, Gd, Dy, Yb, Y) and alkaline earths (Ba, Sr, Ca) were used as a modifier to alumina. The procedure is as follows; The  $\gamma$ - $\text{Al}_2\text{O}_3$  samples added with other elements were prepared by the impregnation of aqueous metal nitrates, and then dried at  $110^\circ\text{C}$  for 8 h, followed by heat-treatment at  $500^\circ\text{C}$  for 3 h in air. Also, the ceria–zirconia ( $\text{CeO}_2$ – $\text{ZrO}_2$ ) for oxygen storage capacity (OSC) was used for the modification to alumina. The compositions were selected at  $(\text{CeO}_2 + \text{ZrO}_2)/\text{Al}_2\text{O}_3 = 0.3/1$  for an OSC catalyst. The  $\text{CuO}_x$  and transition metals (Cr, Mn, Fe, Co, Ni) added catalyst using pure and La-modified alumina as supports were prepared by the same procedure. These catalyst supports and subcatalysts were heated at temperatures of  $800$ – $1200^\circ\text{C}$  for 3 h in air.

The surface areas of the powders were measured from nitrogen adsorption at 77 K after heat treatment at  $200^\circ\text{C}$  under vacuum (Model Autosorp3b, Quantachrome Corp.) by BET (Brunauer–Emmett–Teller) technique. A powder X-ray apparatus (XRD; Model RINT2000, Rigaku Co. Ltd.) with Cu K $\alpha$  source (20 kV–30 mA) was used for the characterization of phases in the samples after heat treatment at various temperatures. The  $\alpha$ -transition temperature ( $T_\alpha$ ) was measured by a differential thermal analysis (DTA, Seiko Instrument DTA30) technique at heating rate of  $10^\circ\text{C}/\text{min}$ . The microscopic or macroscopic morphology was examined by transmission electron microscopy (TEM; JEM-2000EX, JEOL) and scanning (SEM; JSM600, JEOL). Catalytic performance was tested using gas mixtures with a large space velocity of  $100,000\text{ h}^{-1}$ , which simulated automotive exhaust at fuel-lean condition when air/fuel ratio (A/F) was 18. The gas composition and measurement procedure were described in a previous paper [40].

## 3. Results and discussion

### 3.1. Rare earth modification of gamma alumina

Fig. 1 shows the specific surface area of RE-modified alumina powder heated at  $1200^\circ\text{C}$ . The surface area of pure alumina was  $8$ – $12\text{ m}^2/\text{g}$  after heat treatment at  $1200^\circ\text{C}$ , while those of the modified alumina was  $40$ – $70\text{ m}^2/\text{g}$ . The data represent the excellent effect of a series of rare earths as a modifier, which is possible to use regarding present cost level, for the purpose of alumina support stabilization. The data about alkaline earths also indicate the same as rare earths. The heat temperature was selected at  $1200^\circ\text{C}$  for comparison between elements. The results suggest the ionic radius depen-

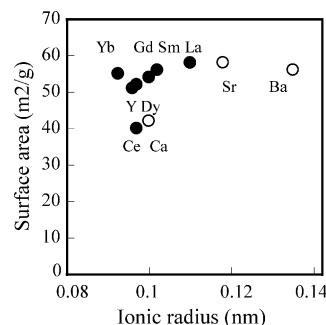


Fig. 1. Specific surface area of alumina support modified with rare earths and alkaline earths followed by heat treatment at  $1200^\circ\text{C}$  for 3 h in air.

dence of these modifiers as stable cations in oxides. However, the performance of surface area stabilization is strongly influenced by the purity and morphology of alumina, as well as rare earth modification process itself for their optimization [3–7].

Lanthanum is actually the most industrial modifier to alumina supports regarding its subcatalytic effect as well as thermal stabilization, which are prepared by several methods in automotive catalysts. The simplest process of rare earth addition is the impregnation, followed by calcination, using aqueous metal salts onto transition alumina (e.g.  $\gamma$ - $\text{Al}_2\text{O}_3$ ) nanoparticles. Besides the direct fabrication of alumina support in industrial large scale, the surface modification using some precipitation agent can be possibly applied to prepare catalysts. The La species can make chemical bond to cover as hydroxide or oxide on alumina surface. The surface coverage of lanthanum oxide as a final form depends on the surface area of alumina and other factors. Practically, the content of a modifier should be selected if the surface area versus concentration is optimized for heat condition used.

Fig. 2 shows the relationship of surface area versus La-content after heat treatment at  $1200^\circ\text{C}$  for comparison of several high surface-area alumina powders. Any alumina has the optimum La-content with relatively low concentration if they are used at  $1000$ – $1200^\circ\text{C}$ . Although  $\text{LaAlO}_3$  is believed to form surface mono-unit layer on alumina [6], it is generally difficult to detect such crystalline states in practical materials.

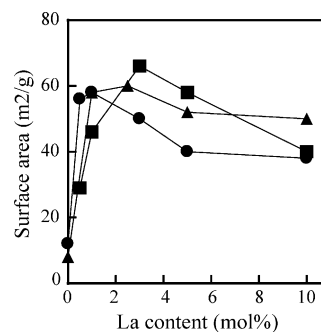


Fig. 2. Relationship of surface area vs. La-content for several alumina powders after heat treatment at  $1200^\circ\text{C}$ . Three marks ( $\blacktriangle$ ,  $\blacksquare$ ,  $\bullet$ ) indicate different raw alumina powders.

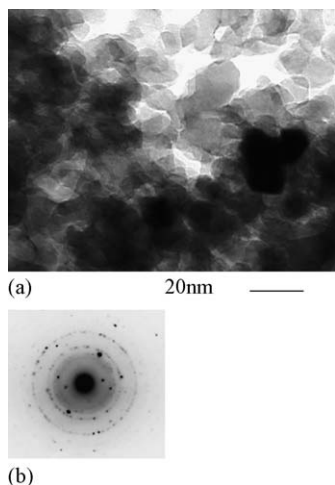


Fig. 3. TEM image of a  $\text{LaAlO}_3$  nanoparticle in 5 mol% La-modified alumina heated at  $1200^\circ\text{C}$  (a) and the electron diffraction pattern (b).

The formation of a layered compound (hexa-aluminate and defective aluminas) by doping small amount of La-cations is possible. Present author has examined the state of trivalent rare earth (Gd and La), which is doped in transition alumina using ESR technique [7]. The other factor is the interaction between nanoparticles, which have hydroxyl group on surface, in agglomeration, as well as particles and species in water. Fig. 3 shows the example of the TEM image in 5 mol% La-modified alumina heated at  $1200^\circ\text{C}$ . A 10 nm size  $\text{LaAlO}_3$  (as a dark-contrast particle) has nucleated in alumina nanoparticulate aggregate matrix when over-loaded La content exists. In the simple impregnation, the La and nitrate species both remains on alumina surface during the drying process, so that an attractive force by the bridging  $\text{La}(\text{NO}_3)_3$  should be active, leading the hard agglomerates of alumina. Such starting state of agglomeration should induce the difference about sintering, phase transformation and solid state reactions in heat treatment. Thus, the La-modification technology is not necessarily settled but still active as an innovative route to improve automotive catalyst.

### 3.2. Alumina-supported ceria–zirconia for OSC

Oxygen storage capacity (OSC) has been a key function in automotive catalysts for precisely controlling the variation of air/fuel ratio in exhaust [10–12]. The optimization of atmosphere in nanospace around catalyst particles leads better efficiencies to remove CO, hydrocarbons and  $\text{NO}_x$ . Also, the oxidation performance may possibly be used for the design of the advanced catalyst for combustion. Ceria–zirconia system has been a standard composition of OSC in high-performance automotive catalyst [13–15,20–31]. The composite (solid solution) subcatalyst is applied to practical three-way catalyst that must have high durability as well as thermal stability [32,33]. In the present work, alumina-supported ceria and ceria–zirconia are examined regarding with the phase and sintering behavior.

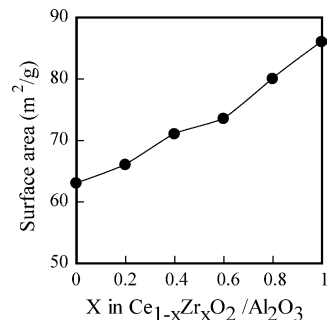


Fig. 4. Specific surface area of  $\text{CeO}_2\text{--ZrO}_2/\text{Al}_2\text{O}_3$  composite powders vs.  $\text{ZrO}_2$ -content, which are prepared by the impregnation method followed by heat treatment at  $800^\circ\text{C}$ .

Fig. 4 shows the specific surface area of  $\text{CeO}_2\text{--ZrO}_2/\text{Al}_2\text{O}_3$  composite powders, which are prepared by the impregnation method, followed by heat treatment at  $800^\circ\text{C}$ . The effect of  $\text{ZrO}_2$  addition on surface area stabilization is evident even in these ordinary  $\text{CeO}_2\text{--ZrO}_2$  subcatalysts. The dependence of surface area versus  $\text{ZrO}_2$ -content suggests the inhibition effect of  $\text{ZrO}_2$  on the grain growth in the impregnation–calcination stage for a series of  $\text{CeO}_2\text{--ZrO}_2$  OSC powders. Since the content of  $\text{CeO}_2\text{--ZrO}_2$  is fairly large per support, the excess fraction should exist out of surface of alumina nanoparticles, while a part of them was coated on surface. Although the influence of nanoparticulate alumina in the impregnation solution is the same as its support, the interaction between  $\text{CeO}_2\text{--ZrO}_2$  and  $\text{Al}_2\text{O}_3$  is found to have specially induced an inhibition behavior on sintering. Thus, the system of  $\text{CeO}_2\text{--ZrO}_2\text{--Al}_2\text{O}_3$  is potentially useful for non-sinterable OSC component as its original form in three-way catalyst.

Fig. 5 shows the XRD patterns of composite powders,  $\text{CeO}_2\text{--ZrO}_2\text{--Al}_2\text{O}_3$ , which were heated at  $800^\circ\text{C}$  in air. A part of  $\text{CeO}_2\text{--ZrO}_2$  seemed to make solid solution; however,

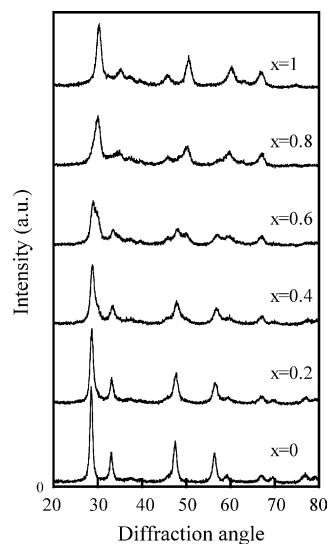


Fig. 5. XRD patterns of a series of composite powders  $(\text{CeO}_2)_{1-x}(\text{ZrO}_2)_x/\text{Al}_2\text{O}_3$  heated at  $800^\circ\text{C}$  for 5 h in air.

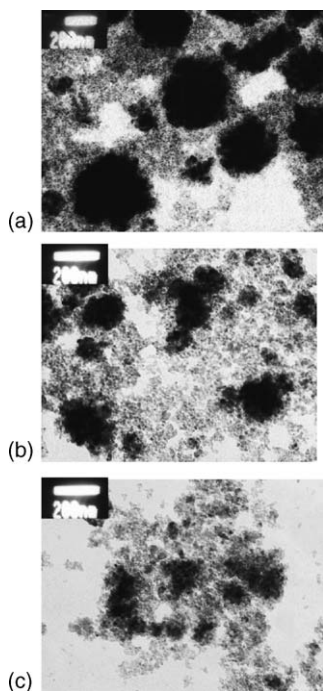


Fig. 6. TEM images of  $\text{CeO}_2\text{-ZrO}_2/\text{Al}_2\text{O}_3$  composite powders heated at  $800^\circ\text{C}$ . (a)  $x=0$ , (b)  $x=0.2$ , (c)  $x=0.6$  in  $(\text{CeO}_2)_{1-x}(\text{ZrO}_2)_x$ .

the complete mixing as a level of crystal lattice was difficult by this process. In the simple impregnation–calcination process, the  $\text{CeO}_2\text{-ZrO}_2$  formed the mixed phase of two partial solid solutions both in  $\text{CeO}_2$ -rich and  $\text{ZrO}_2$ -rich side. Fig. 6 shows the TEM images of several  $\text{CeO}_2\text{-ZrO}_2/\text{Al}_2\text{O}_3$  composite powders heated at  $800^\circ\text{C}$ . The morphology of impregnated composites depends on the ratio of Ce/Zr, in which the spheluric agglomeration of  $\text{CeO}_2\text{-ZrO}_2$  is bedded in the matrix of  $\text{Al}_2\text{O}_3$  network. The aggregate size of  $\text{CeO}_2\text{-ZrO}_2$  decreased with the increase of  $\text{ZrO}_2$  content. Thus, the dispersion with submicron scale can be simply controlled by the addition of  $\text{ZrO}_2$ . This should influence the sintering when the extremely high-temperature exhaust come on these subcatalysts, which must support Pt nanoparticles. It was suggested to behave as full reversible redox between Ce(4+) and Ce(3+) in mid-composition of  $\text{CeO}_2\text{-ZrO}_2$ , leading the better performance as the OSC material [21–26]. On the other hand, from an aspect of total material design, the non-sinterable composite powders are also important. The practical catalytic materials must be subjected to heat condition of exhaust at moderate and high temperatures of  $800\text{--}1100^\circ\text{C}$ , depending on engine operation mode. There is often the trade-off relationship between an atomically structured crystal and practical nanoparticulate heterogeneous catalyst with high surface area. The present results suggest the effect of co-addition from the material design of catalysts, regarding with the sinterability of  $\text{CeO}_2\text{-ZrO}_2$  subcatalyst. The more detailed solid-state characterization and OSC of them will be described in other papers.

Table 1  
 $\alpha$ -Transition temperature of transition metal impregnated alumina catalysts

Element	Pure alumina $T_\alpha$ ( $^\circ\text{C}$ )	La-modified alumina $T_\alpha$ ( $^\circ\text{C}$ )
–	1280	1410
Cr	1240	1380
Mn	1050	1180
Fe	1015	1190
Co	1205	1320
Ni	1225	1300
Cu	1075	1205

The effect of La-modification is compared by DTA at a heating rate of 10 K/min.

### 3.3. La-modified transition metal-doped alumina for de- $\text{NO}_x$ catalyst

The knowledge of solid-state thermal behavior in the systems of alumina and transition metal oxides should be significant in the developments of base (not precious) metal-containing catalysts, but there are not many references so far [34–39]. Also, the effect of co-addition of rare earth and transition metals on alumina at elevated temperatures was less examined. Table 1 compares  $\alpha$ -transition temperature,  $T_\alpha$  of pure  $\gamma\text{-Al}_2\text{O}_3$  (99.995 wt.% purity,  $138\text{ m}^2/\text{g}$ , from Sumitomo Chemical, AKPG015) and La-modified  $\gamma\text{-Al}_2\text{O}_3$  (through impregnation) with 10 mol% transition-metals M (M = Cr, Mn, Fe, Co, Ni, Cu). The data were derived from the starting temperature of exothermal  $\alpha$ -transition peak in DTA curves measured at a heating rate of 10 K/min. In general, such transition metal addition induced a large decrease of transition temperature. The addition of Fe, Mn or Cu has actually resulted in the large decrease of  $T_\alpha$  over  $200^\circ\text{C}$ , while other metals indicated smaller effects to the decrease of  $T_\alpha$  about  $20\text{--}100^\circ\text{C}$ . The XRD detected  $\alpha\text{-Al}_2\text{O}_3$ ,  $\theta\text{-Al}_2\text{O}_3$ ,  $\gamma\text{-Al}_2\text{O}_3$  and complex oxides depending on the sort of impregnated metals in present temperature-range. As known,  $\gamma\text{-Al}_2\text{O}_3$  transforms with increasing temperature, as  $\gamma \rightarrow \delta \rightarrow \theta \rightarrow \alpha$ . There were several features of formed phases via solid-state reactions, depending on species of transition elements. Table 1 indicates that the  $T_\alpha$ (s) are elevated by the La pre-modification leading the thermal stability of transition metal catalysts supported on alumina. The La-modified alumina showed no or little decrease of  $T_\alpha$  even if the transition metals of 10 mol% were impregnated. This is also indicated by the surface area and activity measurement, e.g. in the  $\text{CuO}_x\text{-Al}_2\text{O}_3$  catalyst, as described below.

Fig. 7 compares the typical performance of the NO and  $\text{C}_3\text{H}_6$  removal on  $\text{CuO}_x\text{-Al}_2\text{O}_3$  (heated at 900 and  $1000^\circ\text{C}$ ) and  $\text{CuO}_x\text{-LaO}_x\text{-Al}_2\text{O}_3$  (heated at  $1000^\circ\text{C}$ ) for a model lean–burn exhaust at  $\text{A/F} = 18$  with  $\text{SV} = 100,000\text{ h}^{-1}$ . There seemed to be low efficiencies; however, those were heated at  $1000^\circ\text{C}$  (where any zeolite catalyst shows no activity) for 3 h in air before the measurement. The relationship of NO conversion versus temperature for lean–burn model exhaust showed the same tendency as zeolite catalysts before heat treatment at  $>800^\circ\text{C}$ , indicating the conversion maximum at a certain temperature and the decrease

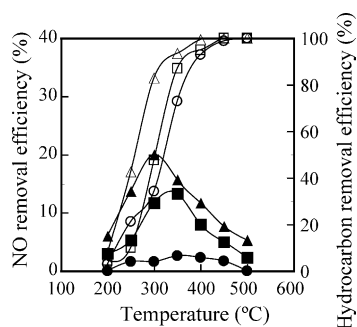


Fig. 7. NO and C<sub>3</sub>H<sub>6</sub> removal efficiencies vs. temperature on CuO<sub>x</sub>-Al<sub>2</sub>O<sub>3</sub> catalyst (heated at 900 and 1000 °C) and CuO<sub>x</sub>-LaO<sub>x</sub>-Al<sub>2</sub>O<sub>3</sub> catalyst (heated at 1000 °C) for a model lean-burn exhaust at A/F=18 with SV=100,000 h<sup>-1</sup>. Removal efficiencies of C<sub>3</sub>H<sub>6</sub> (Δ) and NO (▲) on CuO<sub>x</sub>/Al<sub>2</sub>O<sub>3</sub> (=10/100) heated at 900 °C. Removal efficiencies of C<sub>3</sub>H<sub>6</sub> (○) and NO (●) on CuO<sub>x</sub>/Al<sub>2</sub>O<sub>3</sub> (=10/100) heated at 1000 °C. Removal efficiencies of C<sub>3</sub>H<sub>6</sub> (□) and NO (■) on CuO<sub>x</sub>/LaO<sub>x</sub>/Al<sub>2</sub>O<sub>3</sub> (=10/5/100) heated at 1000 °C.

with increasing temperature. Fig. 8 shows the NO and hydrocarbon (C<sub>3</sub>H<sub>6</sub>) removal efficiencies depending on La-content in La-stabilized CuO<sub>x</sub>-Al<sub>2</sub>O<sub>3</sub>. The Cu 10 mol%-La 5 mol%-co-doped Al<sub>2</sub>O<sub>3</sub> catalyst subjected to heat-treatment at 1000 °C in air maintained the NO removal efficiencies of 14%. The BET surface areas of for alumina catalysts heated were 42 (CuO<sub>x</sub>/LaO<sub>x</sub>/Al<sub>2</sub>O<sub>3</sub> = 10/5/100, heated at 1000 °C), 35 (CuO<sub>x</sub>/Al<sub>2</sub>O<sub>3</sub> = 10/100, heated at 900 °C) and 3 m<sup>2</sup>/g (CuO<sub>x</sub>/Al<sub>2</sub>O<sub>3</sub> = 10/100, heated at 1000 °C), respectively. Although the solid-state reactions are actually complex, the surface area stabilization effect of lanthanum is confirmatively active on CuO<sub>x</sub>-Al<sub>2</sub>O<sub>3</sub> de-NO<sub>x</sub> catalyst. Although de-NO<sub>x</sub> reaction proceeds at 300–700 °C with selective catalytic reduction (SCR) mechanism in engine combustion, the abnormal burning sometimes induces the heat degeneration of catalyst. Fig. 8 shows the optimization of La-content at 5 mol% to CuO<sub>x</sub>/Al<sub>2</sub>O<sub>3</sub> (=10/100) catalyst. This catalyst is an example of the stabilized de-NO<sub>x</sub> catalyst for general purpose by using the rare earth modification of CuO<sub>x</sub>-Al<sub>2</sub>O<sub>3</sub> system, which is enhanced by automotive technology [40–43].

### 3.4. Morphology stabilization of alumina coat layer

Finally, an aspect of ceramics is applied to a thermal stable catalyst washcoat layer. The sintering of catalyst layers was

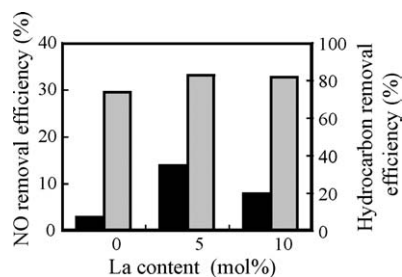


Fig. 8. Dependence of La-content on NO (■) and C<sub>3</sub>H<sub>6</sub> (□) removal performance of CuO<sub>x</sub>/LaO<sub>x</sub>/Al<sub>2</sub>O<sub>3</sub> (=10/0–10/100) after heat treatment at 1000 °C.

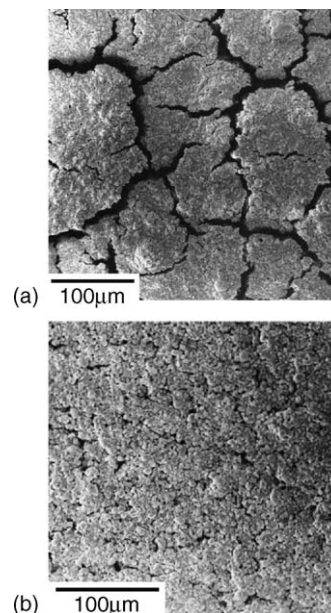


Fig. 9. SEM image of surface morphology on (a) pure Al<sub>2</sub>O<sub>3</sub> and (b) La-modified Al<sub>2</sub>O<sub>3</sub>, which were coated on an alloy thin foil and then heated at 1100 °C for 3 h in air.

related to the grain growth and phase evolution in alumina support. So called “sintering” of ceramics, in this case, has resulted in the fracture of washcoat layers. A larger shrinkage of porous alumina than that of the honeycomb substrate in automotive catalyst is induced by high-temperature exhaust, leading a local stress to form cracks. Fig. 9 shows the SEM image of pure Al<sub>2</sub>O<sub>3</sub> and LaO<sub>x</sub>-Al<sub>2</sub>O<sub>3</sub>, coated on a practical alloy substrate and then heated at 1100 °C for 3 h in air. No critical fracture was found if alumina has been stabilized with La, although some fair cracks are observed. In practice, the rheology of alumina suspension must be controlled during the preparation process of the porous, stable and homogeneous thick coat layer on alloy or ceramic substrates. After then, the La-modified composite alumina will become stable support (as washcoat layer) on an automotive honeycomb bed even subjected to high-heat environment. The strength of agglomerates in powders often prepared by a chemical route is controlled by the extent of particle–particle interaction [44]. Aside from several forces, such as hydrogen bonding to surface hydroxyl groups, the size of units (the primary nanoparticle size) should be the important factor in forming bridges between adjacent particles. La modification stabilizes the nanoparticles by the inhibition of grain growth as well as the metastable phase of alumina below α-transition temperature. This effect leads the macroscopic morphology stabilization of coated layers of alumina at high temperatures. The local perturbation caused by rapid grain growth leads to shrinkage, and consequently, the microstructure drastically evolves when the shrinkage is large. The details on the microdynamics of powder and sintering await more research. The microstructural stabilization technology with rare earth (e.g. La) modification to alumina will be more applied

to the advanced materials of high-temperature exhaust catalyst.

#### 4. Summary

Several results were described as the examples of the high potential of rare earth modification in alumina-based catalyst as well as support. They are summarized as following.

- (1) The surface modification using rare earths to alumina lead better heat-stable catalytic support with nanometer-order particles. The surface area of alumina become over  $60 \text{ m}^2/\text{g}$  at  $1200^\circ\text{C}$ , even through a simple impregnation process.
- (2) The aggregate size of  $\text{CeO}_2\text{-ZrO}_2$  decreased with the increase of  $\text{ZrO}_2$  content so that the dispersion with sub-micron scale can be simply controlled by the addition of  $\text{ZrO}_2$ . The alumina-supported zirconia–ceria subcatalysts for oxygen storage capacity is controlled by the resultant microstructures where the nanoparticles are mixed and rearranged each other after heat treatment.
- (3) The effect of the La pre-modification on the thermal stability of transition metal catalysts was evident. Using this effect, the La-modified, transition metals-promoted alumina catalyst, e.g.  $\text{CuO}_x\text{-La-Al}_2\text{O}_3$  is developed as an inexpensive de- $\text{NO}_x$  catalyst with heat stability.
- (4) La-modified alumina become stable washcoat layer on an alloy foil, which has no cracks at  $1100^\circ\text{C}$ , after the optimized coating process of suspension.

The present work emphasizes the importance of rare earths and their arrangement in these catalytic components from aspect of material design toward thermal stabilization of catalysts.

#### Acknowledgement

A part of work was supported by a foundation grant-in-aid for scientific research, No. 16550167 of the Japanese Ministry of Education, Science, Sports, and Culture.

#### References

- [1] P. Nortier, M. Soustelle, in: Crucq, A. Frennet (Eds.), *Catalysis and Automotive Pollution Control*, Elsevier Science Publisher B.V., Amsterdam, 1987, pp. 275–300.
- [2] N. Miyoshi, S. Matsumoto, M. Ozawa, M. Kimura, SAE paper series 89190, 1989, pp. 1–8.
- [3] D.L. Trimm, *Appl. Catal.* 7 (1983) 249.
- [4] H. Schaper, E.B.M. Doesburg, L.L. Reijin, *Appl. Catal.* 7 (1983) 211.
- [5] P. Buin, J.P. Brunelle, M. Pijolat, M. Soustelle, *Appl. Catal.* 34 (1987) 225.
- [6] F. Oudet, P. Courtine, A. Vejux, *J. Catal.* 114 (1988) 112.
- [7] M. Ozawa, M. Kimura, A. Isogai, *J. Less-Common Met.* 162 (1990) 297.
- [8] M. Ozawa, M. Kimura, A. Isogai, US patent No. 4722920, 1988.
- [9] M. Ozawa, Y. Nishio, *J. Alloys Compd.* 374 (2004) 397.
- [10] H.S. Gandhi, A.G. Piken, M. Shelef, R.G. Delosh, SAE paper No.760201, 1976.
- [11] H.C. Yao, Y.F. Yao, *J. Catal.* 86 (1984) 254.
- [12] T. Miki, T. Ogawa, M. Haneda, N. Kakuta, A. Ueno, S. Tateishi, S. Matsuura, M. Sato, *J. Phys. Chem.* 94 (1990) 6464.
- [13] M. Ozawa, M. Kimura, A. Isogai, S. Matsumoto, N. Miyoshi, US patent No. 5075276, 1990.
- [14] M. Ozawa, M. Kimura, A. Isogai, *J. Alloys Compd.* 193 (1993) 73.
- [15] T. Murota, T. Hasegawa, S. Aozasa, H. Motoyama, M. Matsui, *J. Alloys Compd.* 193 (1993) 298.
- [16] H. Tanaka, M. Uenishi, I. Tan, M. Kimura, J. Mizuki, Y. Nishihata, SAE paper, SP-1573, 2001, p. 123.
- [17] N. Sato, H. Tanaka, I. Tan, M. Uenishi, N. Kajita, M. Taniguchi, SAE paper, SP-1756, 2003, p. 31.
- [18] H. Tanaka, M. Taniguchi, I. Tan, N. Kajita, M. Uenishi, K. Kaneko, C. Mitate, *Jpn. Kokai Tokkyo Koho* (2004) JP2004181435.
- [19] M. Ozawa, M. Kimura, A. Isotani, US patent No. 4921829, 1990.
- [20] C. de Leitenburg, A. Trovarelli, F. Zamar, S. Maschio, G. Dolcetti, J. Llorca, *J. Chem. Soc., Chem. Commun.* (1995) 2181.
- [21] J.-P. Cuif, G. Blanchard, O. Touret, M. Marczy, E. Quemere, SAE paper, SP-1207, 1996, p. 73.
- [22] F. Zamar, A. Trovarelli, C. de Leitenburg, G. Dolcetti, *Stud. Surf. Sci. Catal.* 101 (1996) 1283.
- [23] H. Permana, D.N. Belton, K.M. Rahmoeller, S. Schmiege, C.E. Hori, K.Y. Ng, A. Brenner, SAE paper, SP-1288, 1997, p. 23.
- [24] G. Balducci, J. Kaspar, P. Fornasiero, M. Graziani, M.S. Islam, J.D. Gale, *J. Phys. Chem. B* 101 (1997) 1750.
- [25] M. Ozawa, *J. Alloys Compd.* 257–277 (1998) 886.
- [26] M. Sugiura, *Catal. Survey Asia* 7 (2003) 77.
- [27] M. Sugiura, M. Ozawa, A. Suda, T. Suzuki, T. Kanazawa, *Bull. Chem. Soc. Jpn.* 78 (2005) 752–767.
- [28] M.H. Yao, R.J. Baird, F.W. Kunz, T.E. Hoost, *J. Catal.* 166 (1997) 67.
- [29] M. Ozawa, K. Matuda, S. Suzuki, *J. Alloys Compd.* 303/304 (2000) 56.
- [30] M. Ozawa, C.-K. Loong, *Catal. Today* 50 (1999) 329.
- [31] R. Di Monte, P. Fornasiero, J. Kaspar, M. Graziani, *Stud. Surf. Sci. Catal.* 140 (2001) 229.
- [32] A. Kozlov, D.H. Kim, A. Yezerets, P. Andersen, H.H. Kung, M.C. Kung, *J. Catal.* 209 (2002) 417.
- [33] T. Kanazawa, J. Suzuki, T. Takada, T. Suzuki, A. Morikawa, A. Suda, H. Sobukawa, M. Sugiura, SAE paper, SP-1756, 2003, p. 17.
- [34] G.C. Bye, G.T. Simpkin, *J. Am. Ceram. Soc.* 57 (1974) 367.
- [35] Y. Wakao, T. Hibino, *Nagoya-Kogyo-Gijutu-shikensho-Houkoku* 11 (1962) 588.
- [36] M. Ozawa, O. Kato, S. Suzuki, Y. Hattori, M. Yamamura, *J. Mater. Sci. Lett.* 15 (1996) 564.
- [37] M. Ozawa, O. Kato, S. Suzuki, *J. Mater. Sci.* 33 (1998) 737.
- [38] M. Ozawa, K. Hashimoto, S. Suzuki, *J. Mater. Sci.* 36 (2001) 1401.
- [39] M. Ozawa, H. Kato, S. Suzuki, *J. Mater. Sci.* 38 (2003) 2607.
- [40] M. Ozawa, H. Toda, O. Kato, S. Suzuki, *Appl. Catal. B* 8 (1996) 122.
- [41] M. Ozawa, H. Toda, S. Suzuki, *Appl. Catal. B* 8 (1996) 141.
- [42] M. Ozawa, C.-K. Loong, *Physica B* 241/242 (1998) 269.
- [43] M. Ozawa, M. Ito, S. Suzuki, *J. Mater. Sci.* 33 (1998) 4717.
- [44] M. Ozawa, S. Suzuki, H. Toda, *J. Am. Ceram. Soc.* 80 (1997) 1957–1964.